International Scholarly Research Network
ISRN Physical Chemistry
Volume 2012, Article ID 781879, 7 pages
doi:10.5402/2012/781879

Research Article

A Novel Poly{(2,5-diyl furan) (benzylidene)}: A New Synthetic Approach and Electronic Properties

Abdelkader Belmokhtar,[1] Ahmed Yahiaoui,[1] Aïcha Hachemaoui,[1] Benyoucef Abdelghani,[1] Nabahat Sahli,[2] and Mohammed Belbachir[2]

[1] *Laboratoire de Chimie Organique, Macromoléculaire et des Matériaux (LCOMM), Faculté des Sciences et de la Technologie, Université de Mascara, P.O. Box 763, Mascara 29000, Algeria*
[2] *Laboratoire de Chimie des Polymères, Faculté des Sciences, Université d'Oran, P.O. Box 1524, El-Menouer 31000, Algeria*

Correspondence should be addressed to Ahmed Yahiaoui, yahmeddz@yahoo.fr

Received 6 September 2011; Accepted 28 September 2011

Academic Editors: J. M. Farrar, J. G. Han, and L. Vattuone

A new conjugated aromatic poly[(furan-2, 5-diyl)-co-(benzylidene)] has been prepared by polycondensation of benzaldehyde and furan catalyzed by Maghnite-H^+. Maghnite-H^+ is a montmorillonite sheet silicate clay, which exchanged with protons. These polymers can be dissolved in high polar solvents such as DMSO, DMF, THF, or $CHCl_3$ A kind of band-gap conjugated poly[(furan-2, 5-diyl)-co-(benzylidene)] has been synthesized by a simple method and characterized by ^{1}HNMR, ^{13}CNMR, FT-IR, and UV-Vis. The result reveals that the band-gap of the PFB conjugated polymer has an optical band gap of 2.2 eV.

1. Introduction

Intensive research efforts in the field of organic photovoltaics during the last 15 years has resulted in a gradual improvement of the efficiencies of organic solar cells, up to the level of 4–6% achieved during the period 2005–2008 [1–8]. The discovery of electrical conductivity of organic conjugated polymers has opened a novel and very important field of modern functional material science. In the past few years, a conducting polyaniline (PAN) has been the center of great interest because of its high electrical conductivity and chemical stability [9–11]. The discovery of electrical conductivity of organic conjugated polymers has opened a novel and very important field of modern functional material science. The heterocyclic polymers, such as polypyrrole and polythiophene, have also received a great deal of interest due to their high conductivity in the doped state accompanied by a much higher stability in air [9–13]. However, polyfuran has attracted relatively less attention because the polyfuran with a regular structure and high conductivity was synthesized with difficulty.

Recently, an Algerian proton exchanged montmorillonite clay called Maghnite-H^+ (Mag-H^+), a new nontoxic cationic initiator, was used as a catalyst for cationic polymerization of a number of vinylic and heterocyclic monomers [14–16].

In the present work, we present a new approach to design poly[(furan-2,5-diyl)-co-(benzylidene)] (PFB) in one shot, namely, by the condensation of furan and benzaldehyde catalyzed by Mag-H^+ (Figure 1). In contrast to most of the other conductive polymers, PFB is a soluble polymer in commons organic solvents. The catalyst can be easily separated from the polymer product and regenerated by heating at a temperature above 0°C. The effects of different synthesis parameters, such as the amount of Mag-H^+, temperature, monomer, furan, and benzaldehyde are discussed.

2. Experimental

2.1. Materials. Furan was purchased from Aldrich Chemical Co. and distilled under reduced pressure. Dichloromethane and benzaldehyde were used as received. The molecular

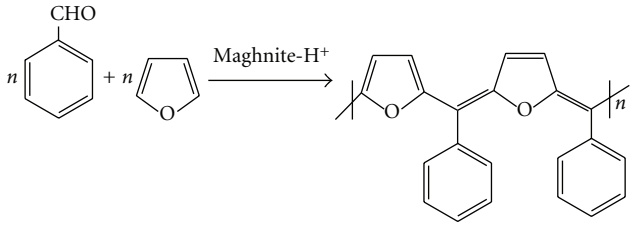

Figure 1: The synthetic route of poly[(furan-2,5-diyl)-co-(benzylidene)] (PFB) by Mag-H^+ catalyst.

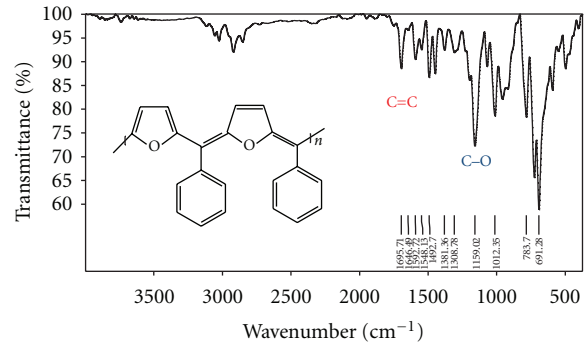

Figure 2: FT-IR spectrum of poly[(furan-2,5-diyl)-co-(benzylidene)] product of the reaction.

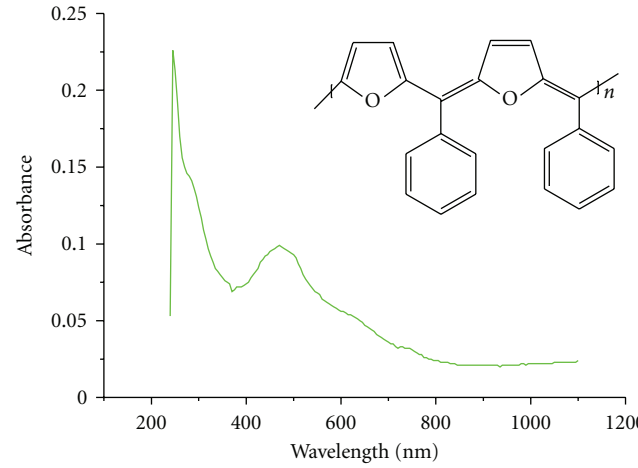

Figure 3: The UV-Vis spectra of poly[(furan-2,5-diyl)-co-(benzylidene)] in CH_2Cl_2.

structure of the polymer was characterized by FT-IR spectroscopy (Perkin-Elmer System).

UV spectra were obtained by an OPTIZEN 2120 UV-Vis spectrometer using the dichloromethane solution of polymers with a concentration of 0, 00125 mg/mL.

^{1}H-nuclear magnetic resonance (NMR), ^{13}C NMR measurements were carried out on a 300 MHz Bruker NMR Spectrometer equipped with a probe BB05 mm, in $CDCl_3$. Tetramethylsilane (TMS) was used as the internal standard in these cases.

2.2. Polymer Preparation. In a 50 mL beaker, furan (6 mmol) and benzaldehyde (6 mmol) were dissolved in 10 mL of 1,2-dichloroethane and a chosen amount of Maghnite-H^+ was added. The weight ratio (Maghnite-H^+/Fu; BA) was kept constant (at the desired value) in all flask. At the end of the reaction, the resulting mixture was filtered to remove the clay and then slowly added to methanol with stirring and then the polymer was dried under vacuum at room temperature for 24 h.

3. Results and Discussion

Most of the PFB were found to be soluble in organic solvents such as tetrahydrofuran (THF), CH_2C1_2, N, N-dimethylformamide (DMF), and sulfolane. Although polymers have highly conjugated chains due to the high degree of dehydrogenation, they were very soluble in organic solvents such as THF, giving grey solutions of high concentrations. The very good solubility of polymers in spite of their high degree of π-conjugation is due largely to the bulky side groups (Φ) at the methane carbon =C (Φ) link and also to the low molecular weight to some extent.

Figure 2 presents the FTIR spectrum of poly[(furan-2,5-diyl)-co-(benzylidene)], that shows the appearance of a strong absorption at 1664 cm^{-1} which is attributed to the stretching vibration of conjugated C=C and the stretching vibration of aromatic in phenylene. A distinct peack near 783 cm^{-1} is due the out of plane vibration C_β–H characteristic of the α-linkage in furan rings. The peak at 1012 cm^{-1} is due the vibration of C–O in furan.

Figure 3 presents the UV-vis spectrum of poly[(furan-2,5-diyl) (benzylidene)] in CH_2Cl_2. Two absorption bands appear in the UV-vis spectrum of the virgin polymer solution in CH_2Cl_2. The strong absorption (band I) at 260 nm is assigned to the π-π^* transition of the furan rings of poly[(furan-2,5-diyl)-co-(benzylidene)] backbone, and a weak absorption (band II) around 500 nm to the n-π^* transition of the quinoid rings [17–19].

In ^{1}H RMN spectrum (Figure 4), the characteristic methine hydrogen resonance at about 5.47 ppm for precursors completely disappeared, but a new proton resonance of 7.2–7.8 ppm was observed, indicating the formation of the quinoid rings in the polymer backbone. The polymers so obtained are readily solution common organic solvents, such as chloroform, dichloromethane, and THF.

In Figure 5, ^{13}C NMR spectrum of the poly[(furan-2,5-diyl)-co-(benzylidene)] exhibits a signal at 140 ppm that can be assigned to the carbon atoms in the α-position on furan units, whereas the signal at 155 ppm is related to the same α-carbons in the terminal furan rings, where the shielding effect is weaker. Moreover, the strongest signal around 128 ppm may be ascribed to the carbon atoms in the poly[(furan-2,5-diyl)-co-(benzylidene)] chains. A similar ^{13}C NMR spectrum of an ordered oligo(furan) has been reported [15]. These findings further confirm that the polyfuran obtained here consists essentially of a π-conjugated structure.

3.1. Effect of the Amount of Mag-H^+. Figure 6 shows the effect of the amount of Mag-H^+, expressed by using various weight

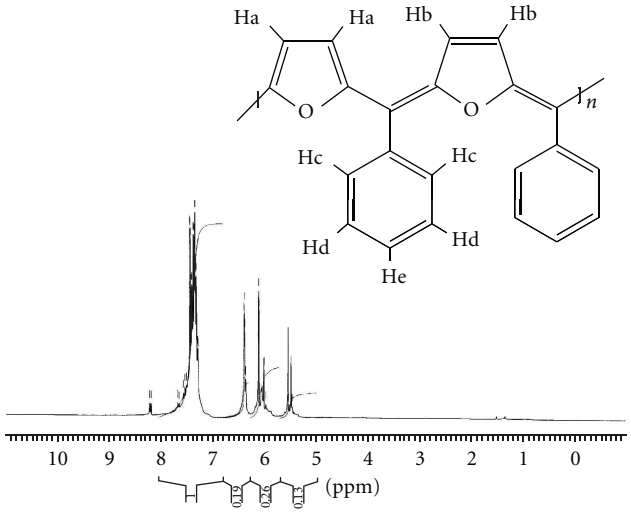

Figure 4: ^{1}H-NMR spectrum (300 MHz) of poly[(furan-2,5-diyl)-co-(benzylidene)] (solvent, $CDCl_3$).

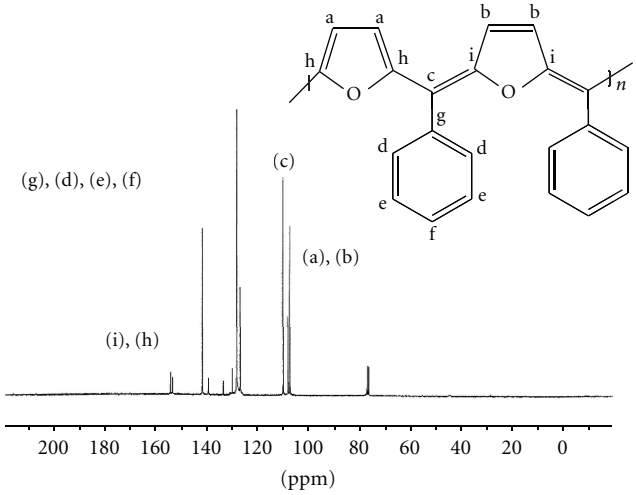

Figure 5: ^{13}C-NMR spectrum (300 MHz) of poly[(furan-2,5-diyl)(benzylidene)] (solvent, $CDCl_3$).

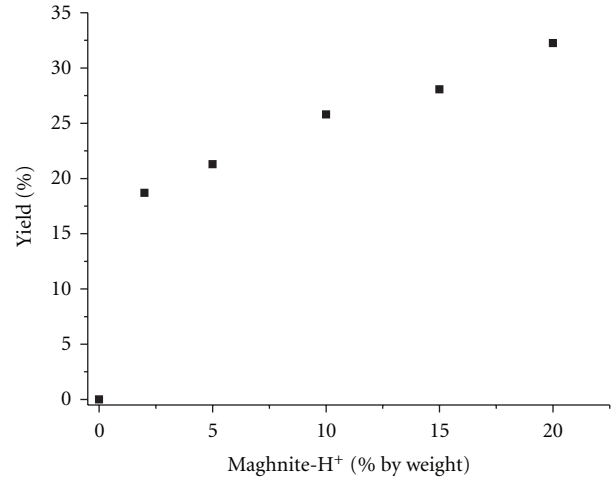

Figure 6: Effect of the amount of Mag-H^+ on the yield of PFB.

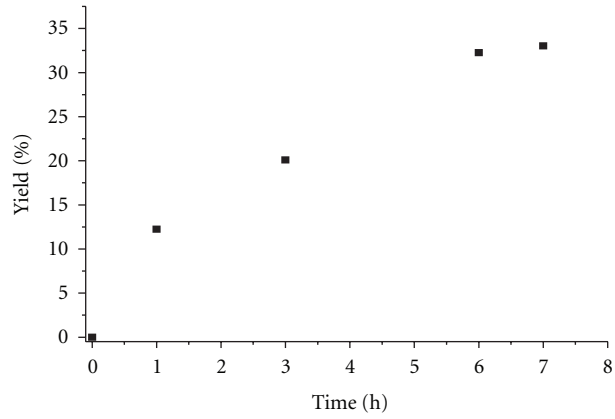

Figure 7: Yield of PPCB at Maghnite-H^+ = 5%, [benzaldehyde] = [furan] = 6×10^{-3} mol/L.

ratios Mag-H^+/monomer, on the polymerization rate. The polymerization was carried out in bulk. The yield of PFB increased with the amount of Mag-H^+, in which the effect of Mag-H^+ as a cationic catalyst for furan and benzaldehyde copolymerization is clearly shown. Similar results are obtained by Yahiaoui et al. [20–22] in the polymerization of epichlorhydrin, propylene oxide and cyclohexene oxide by Mag-H^+ and the polymerization of styrene by montmorillonite, respectively. This phenomenon is probably the result of the number of "initiating active sites" responsible of inducing polymerization, this number is prorating to the catalyst amount used in reaction.

3.2. Effect of Time on Condensation. Figure 7 shows the yield of polymer *versus* time for polymerization of furan using Mag-H^+ as catalyst. As the figure shows, polymerization takes place rapidly and smoothly, reaching a conversion of 32% after 6 h. The polymerization yield became constant at that time; this is probably the result of an increase in the medium viscosity.

3.3. Effect of Temperature on the Polycondensation of Benzaldehyde and Furan. In the presence of Maghnite-H^+ at various weight ratios Maghnite-H^+/monomer, the polycondensation of benzaldehyde and furan was carried out for 180 minutes. The reaction was induced at different temperatures and the effect of temperature on polymerisation was studied. The results are shown in Figure 8. The yield of poly[(furan-2,5-diyl)-co-(benzylidene)] was found to increase with the temperature and it reaches a maximum at 25°C, above this value of temperature the conversion decreases.

Optical Results. When light passes through a medium, its behavior will depend on the proprieties of the medium and of the light (reflection, absorption, refraction and scattering). The refractive index in its real and imaginary parts or dielectric function is the response to interaction between the material and light. To well study these parameters, it is

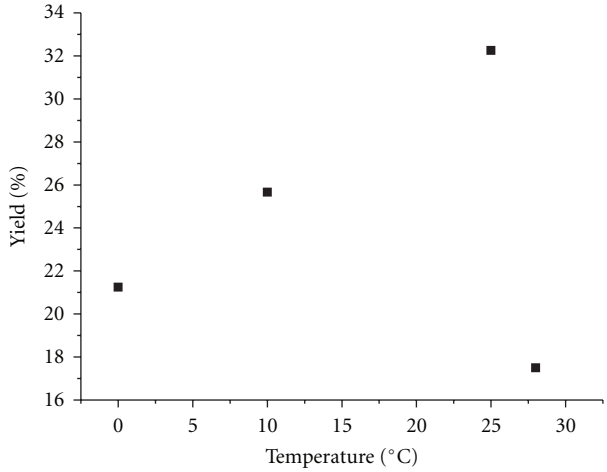

Figure 8: Effect of the temperature on the yield of PFB. Maghnite-H^+ = 5%, t = 6 h.

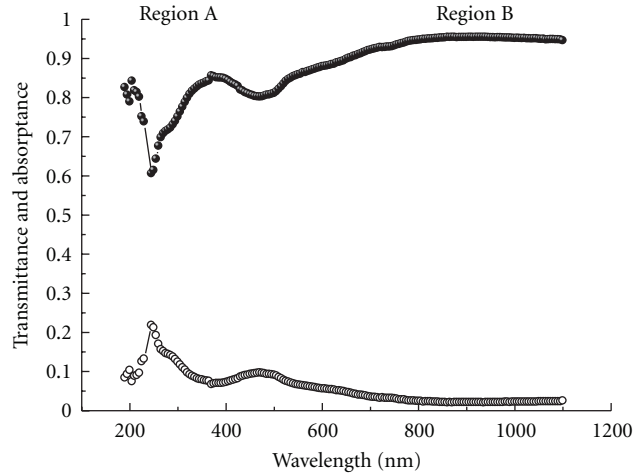

Figure 9: Transmittance and absorptance variation in UV-range.

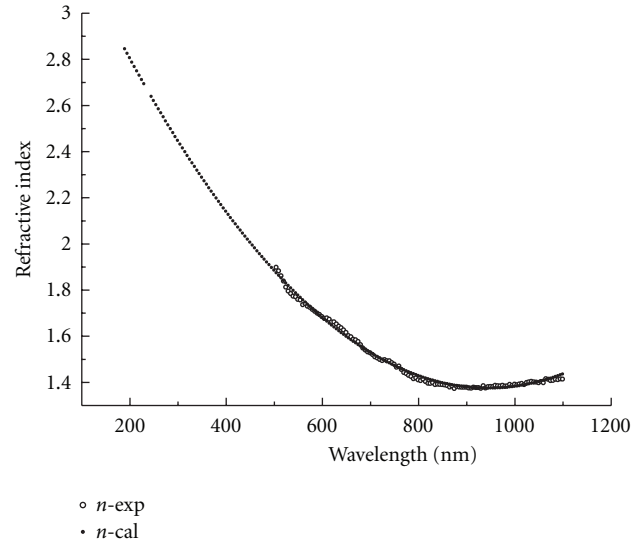

Figure 10: Refractive index variation in UV-range, and simulated curve by Cauchy model.

necessary to make the optical measurements (transmission and/or reflection) in the UV wavelength range. We present in Figure 9 the transmittance T and absorptance A spectra normalized with regard to the basic line in the range wavelength from 190 to 1100 nm [23]. We distinguish clearly two regions in these spectra.

(i) Region A or Absorption Region. In this range the transmittance and absorptance spectra show a strong variation with diminution the transmittance spectrum and increase the level of absorptance. In this range, we can deduce from the transmittance spectra the absorption coefficient $\alpha(\omega)$ at frequency ω, by the following relation [24]:

$$\alpha(\omega) = -\frac{1}{d}\ln[T], \tag{1}$$

where d is the thickness of the film and T its transmittance normalized by background. For the material no dispersive, the reflectance spectrum R is calculated by

$$R = 1 - A - T. \tag{2}$$

(ii) Region B or Transparency Region. In this range of wavelength, the optical transmittance remains practically constant at 0.98 (98%) and the absorptance is typically equal to zero. In this region, we can determined the refractive index n, where R is related to refractive index n for the normally incidence by relation

$$R = \left(\frac{n-1}{n+1}\right)^2. \tag{3}$$

From this expression, we can deduce the refractive index in transparency region:

$$n = \frac{1+\sqrt{R}}{1-\sqrt{R}}. \tag{4}$$

The values found for the refractive index at room temperature for unpolarized light are represented in Figure 10. From the results shown in this figure it clearly appears that the refractive index decrease rapidly (1.9 to 1.4) in the wavelength range from 190 to 500 nm and remains constant in the region between 500 and 1100 nm.

This behavior is in a good agreement with results found for semiconductors such as silicon (Si) and germanium (Ge) [25, 26]. For determining the refractive index in all wavelength range studied, we simulated this parameter by Cauchy model [27]. Cauchy's equation is an empirical relationship between the refractive index n and wavelength λ of light for particular transparent material. The most general form of Cauchy's equation is

$$n(\lambda) = A + \frac{B}{\lambda^2} + \frac{C}{\lambda^4} + \cdots, \tag{5}$$

where $A, B, C, \ldots$, are coefficients that can be determined for a material by fitting the equation to measured refractive

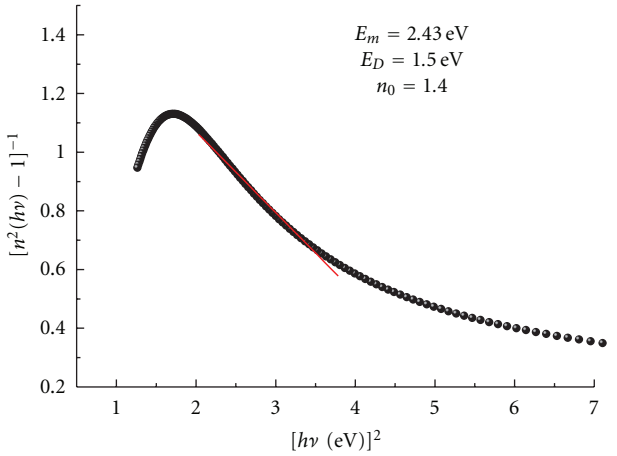

Figure 11: Show the Wemple Didominico model for determined the average gap E_m, dispersion energy E_D, and static refraction index n_0.

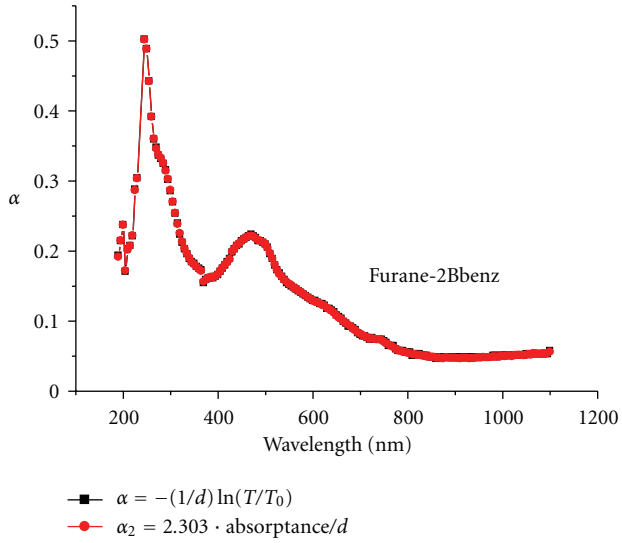

Figure 12: Absorption coefficient, α, obtained from transmission spectra and empirical relation.

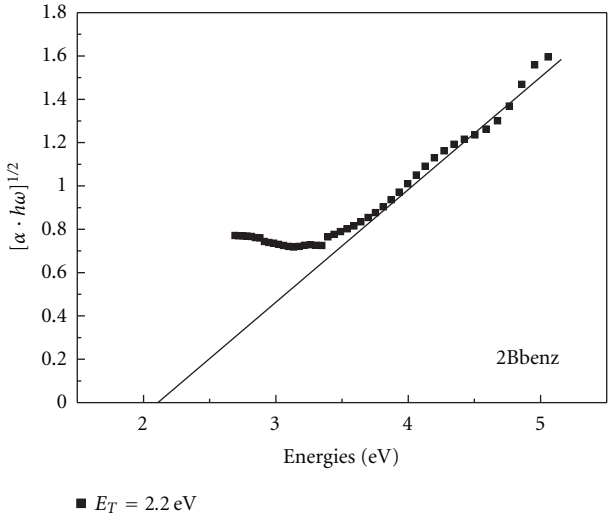

Figure 13: Tauc gap optic, E_{Tauc}, variation separating the extrema of the valence and conduction bands.

indices at known wavelengths. Usually, it is sufficient to use a two term form of the following equation:

$$n(\lambda) = A + \frac{B}{\lambda^2}. \tag{6}$$

We notice that both spectra are perfectly superposed in the high wavelengths range from 500 to 1100 nm. We can by this model generalize the refractive index variation on the low wavelengths range (from 190 to 500 nm). In order to understand this phenomenon well, the values of the static refractive index n_0 (refractive index at zero energy: that is, $n_0 = n\,(\hbar\omega = 0)$) is determined from the analysis of the Wemple and Didominico one oscillator model [28]. According to this model, the dispersion relation of the refractive index is given by

$$n^2(\hbar\omega) = 1 + \frac{E_D \cdot E_m}{E_{m^2} - (\hbar\omega)^2}, \tag{7}$$

where E_m denotes the average gap E_D denotes the dispersion energy related to the coordination number of the atoms. The static refractive index n_0, average gap E_m, and dispersion energy E_D are deduced by considering the variation of $[n^2(\hbar\omega) - 1]^{-1}$ as function of $(\hbar\omega)^2$ (Figure 11). The values obtained for these parameters by this analysis are

$$Em = 2.43\,\text{eV}, \qquad E_D \approx 1.5\,\text{eV}, \qquad n_0 = 1.4. \tag{8}$$

The difference is obtained in values for average gap E_m by these models due principally to prediction of each. Nevertheless, the values found for E_m show clearly that our material is a good semiconductor and can be compared to silicon or germanium, although the value of E_D is relatively lower.

In Figure 12, we represent the variation of absorption coefficient $\alpha(\omega)$ determined by relation (1) and compared it with empirical relation given by

$$\alpha = 2.303\frac{A}{d}. \tag{9}$$

This second relation is valid for a weak reflection on the surface of the film. These conditions are verified well in this range of absorption where the material is absorbent [29]. Figure 12 shows clearly a good agreement between these methods for this material.

From the absorption spectra, we determined the Tauc gap (E_{Tauc}) separating the extrema of the valence and conduction bands supposed parabolic and not perturbed by the disorder, by the extrapolation of the part strong absorption towards the weak energies according to the relation [30]

$$[\hbar\omega \cdot \alpha(\hbar\omega)]^{1/2} = c^{\text{ste}}(\hbar\omega - E_{\text{Tauc}}). \tag{10}$$

In Figure 13, we show this variation and extrapolate the Tauc gap (E_{Tauc}). The value founded for this parameter is equal to

2.2 ± 0.2 eV. This value is nattily lower than the average gap and compared to the good semiconductors, for example, the amorphous silicon and germanium [26].

4. Conclusions

Maghnite-H^+, proton exchanged montmorillonite clay, is an effective initiator for the copolymerization of benzaldehyde with furan.

A novel conjugated aromatic, poly[(furan-2,5-diyl)-co-(benzylidene)], which has a π-conjugated chain was synthesized by Maghnite-H^+. The resultant polymer showed good solubility in common organic solvents and good film formability. Such results may serve primarily to illustrate a new strategy to increase the solubility of low band gap polymers through the arrangement of different aromatic heterocycles in conjugated polymer backbones. The results obtained with optical measurements and analyzed by different models show clearly that our material poly[(furan-2,5-diyl)-co-(benzylidene)] is a good semiconductor, when the optical gap separating the extrema of the valence and conduction bands is around 2.2 ± 0.2 eV. This value goes a good agreement with those found for the semiconductors materials such as Silicon and germanium.

Acknowledgments

This work was supported by The National Agency for the Development of University Research (ANDRU) and the Directorate General of Scientific Research and Technological Development (DGRSDT) of Algeria.

References

[1] H. Hoppe and N. S. Sariciftci, "Organic solar cells: an overview," *Journal of Materials Research*, vol. 19, no. 7, pp. 1924–1945, 2004.

[2] J. Peet, J. Y. Kim, N. E. Coates et al., "Efficiency enhancement in low-bandgap polymer solar cells by processing with alkane dithiols," *Nature Materials*, vol. 6, no. 7, pp. 497–500, 2007.

[3] Y. K. Jin, K. Lee, N. E. Coates et al., "Efficient tandem polymer solar cells fabricated by all-solution processing," *Science*, vol. 317, no. 5835, pp. 222–225, 2007.

[4] K. M. Coakley and M. D. McGehee, "Conjugated polymer photovoltaic cells," *Chemistry of Materials*, vol. 16, no. 23, pp. 4533–4542, 2004.

[5] H. Hoppe and N. S. Sariciftci, "Morphology of polymer/fullerene bulk heterojunction solar cells," *Journal of Materials Chemistry*, vol. 16, no. 1, pp. 45–61, 2006.

[6] H. Hoppe and N. S. Sariciftci, *Advances in Polymer Science*, Springer, Berlin, Germany, 2008.

[7] B. C. Thompson and J. M. J. Frechet, "Polymer fulleren solarzellen," *Angewandte Chemie*, vol. 120, no. 1, pp. 62–82, 2008.

[8] B. C. Thompson and J. M. J. Frechet, "Polymer–fullerene composite solar cells," *Angewandte Chemie*, vol. 47, no. 1, pp. 58–77, 2008.

[9] A. G. MacDiarmid, "'Synthetic metals': a novel role for organic polymers (Nobel lecture)," *Angewandte Chemie*, vol. 40, no. 14, pp. 2581–2590, 2001.

[10] J. Huang and R. B. Kaner, "A general chemical route to polyaniline nanofibers," *Journal of the American Chemical Society*, vol. 126, no. 3, pp. 851–855, 2004.

[11] D. F. Acevedo, M. C. Miras, and C. A. Barbero, "Solid support for high-throughput screening of conducting polymers," *Journal of Combinatorial Chemistry*, vol. 7, no. 4, pp. 513–516, 2005.

[12] Y. C. Liu and K. C. Chung, "Characteristics of conductivity-improved polypyrrole films via different procedures," *Synthetic Metals*, vol. 139, no. 2, pp. 277–281, 2003.

[13] G. M. Abou-Elenien, A. A. El-Maghraby, and G. M. El-Abdallah, "Electrochemical relaxation study of polythiophene as conducting polymer (I)," *Synthetic Metals*, vol. 146, no. 2, pp. 109–119, 2004.

[14] M. Belbachir and A. Bensaoula, "Composition and method for catalysis using bentonites," US Patent, no. 6274527, 2006.

[15] R. Meghabar, A. Megherbi, and M. Belbachir, "Maghnite-H^+, an ecocatalyst for cationic polymerization of *N*-vinyl-2-pyrrolidone," *Polymer*, vol. 44, no. 15, pp. 4097–4100, 2003.

[16] M. I. Ferrahi and M. Belbachir, "Polycondensation of tetrahydrofuran with phthalic anhydride induced by a proton exchanged montmorillonite clay," *International Journal of Molecular Sciences*, vol. 4, no. 6, pp. 312–325, 2003.

[17] A. Gok, B. Sari, and M. Talu, "Chemical preparation of conducting polyfuran/poly(2-chloroaniline) composites and their properties: a comparison of their components, polyfuran and poly(2-chloroaniline)," *Journal of Applied Polymer Science*, vol. 88, no. 13, pp. 2924–2931, 2003.

[18] X. G. Li, R. Liu, and M. R. Huang, "Facile synthesis and highly reactive silver ion adsorption of novel microparticles of sulfodiphenylamine and diaminonaphthalene copolymers," *Chemistry of Materials*, vol. 17, no. 22, pp. 5411–5419, 2005.

[19] X. G. Li, M. R. Huang, and S. X. Li, "Facile synthesis of poly(1, 8-diaminonaphthalene) microparticles with a very high silver-ion adsorbability by a chemical oxidative polymerization," *Acta Materialia*, vol. 52, no. 18, pp. 5363–5374, 2004.

[20] A. Yahiaoui, M. Belbachir, and A. Hachemaoui, "An acid exchanged montmorillonite clay-catalyzed synthesis of polyepichlorhydrin," *International Journal of Molecular Sciences*, vol. 4, no. 10, pp. 548–561, 2003.

[21] A. Yahiaoui, M. Belbachir, and A. Hachemaoui, "Cationic polymerization of 1, 2-epoxypropane by an acid exchanged montmorillonite clay in the presence of ethylene glycol," *International Journal of Molecular Sciences*, vol. 4, no. 11, pp. 572–585, 2003.

[22] A. Yahiaoui, M. Belbachir, J. C. Soutif, and L. Fontaine, "Synthesis and structural analyses of poly (1, 2-cyclohexene oxide) over solid acid catalyst," *Materials Letters*, vol. 59, no. 7, pp. 759–767, 2005.

[23] C. Manfredotti, F. Fizzotti, M. Boero, P. Pastorino, P. Polesello, and E. Vittone, "Influence of hydrogen-bonding configurations on the physical properties of hydrogenated amorphous silicon," *Physical Review B*, vol. 50, no. 24, pp. 18046–18053, 1994.

[24] N. M. Ahmed, Z. Sauli, U. Hashim, and Y. Al-Douri, "Investigation of the absorption coefficient, refractive index, energy band gap, and film thickness for $Al_{0.11}Ga_{0.89}N$, $Al_{0.03}Ga_{0.97}N$, and GaN by optical transmission method," *International Journal of Nanoelectronics and Materials*, vol. 2, pp. 189–195, 2009.

[25] Y. Bouizem, A. Belfedal, J. D. Sib, A. Kebab, and L. Chahed, "Hydrogen-bonding configuration effects on the optoelectronic properties of glow discharge a-$Si_{1-x}Ge_x$:H with large x," *Journal of Physics: Condensed Matter*, vol. 19, no. 25, p. 356215, 2007.

[26] Y. Bouizem, A. Belfedal, J. D. Sib, A. Kebab, and L. Chahed, "Optoelectronic properties of hydrogenated amorphous germanium deposited by rf-PECVD as a function of applied rf-power," *Journal of Physics Condensed Matter*, vol. 17, no. 33, pp. 5149–5158, 2005.
[27] A. L. Cauchy, "Mémoire sur la théorie de la lumière," *Belletin des Sciences Mathematiques*, vol. 14, no. 6, 1830.
[28] S. H. Wemple and M. DiDomenico, "Behavior of the electronic dielectric constant in covalent and ionic materials," *Physical Review B*, vol. 3, no. 4, pp. 1338–1351, 1971.
[29] P. Tyagi and A. G. Vedeshwar, "Grain size dependent optical band gap of CdI2 films," *Bulletin of Materials Science*, vol. 24, no. 3, pp. 297–300, 2001.
[30] J. Tauc and A. Meuth, "A perturbation analysis of non-linear free flexural vibrations of a circular cylindrical shell," *Journal of Non-Crystalline Solids*, vol. 8–10, no. 4, pp. 569–585, 1972.